JOURNAL OF SOLID STATE CHEMISTRY 2, 612–618 (1970)

The Crystal Structure of Magnesium Germanate: A Reformulation of Mg_4GeO_6 as $Mg_{28}Ge_{10}O_{48}$

R. B. VON DREELE,† P. W. BLESS, E. KOSTINER AND R. E. HUGHES

Department of Chemistry, Cornell University, Ithaca, New York, 14850

Received July 29, 1970

Single crystals of magnesium germanate were obtained from a lead oxide flux crystallization of a ceramic preparation from an initial charge of $4MgO \cdot GeO_2$. The crystals are orthorhombic with $a = 14.512(2)$, $b = 10.219(2)$, and $c = 5.944(1)$ and the unit cell contents, $Mg_{28}Ge_{10}O_{48}$, conform to the symmetry requirements of the space group *Pbam*. The crystal structure was accurately determined by X-ray diffraction analysis with a final residual $R = 0.044$. The structure, which is based upon a closest packed oxygen anion array, $(ABACBC)_n$, involves a unique stacking of an olivine-type layer with a substituted MgO-type layer.

Introduction

A magnesium germanate of reported composition, Mg_4GeO_6, occurs in the magnesium oxide–germanium dioxide system as a stable phase up to a temperature of $1495 \pm 10°C$, above which it dissociates to the forsterite form of Mg_2GeO_4 and MgO (*1*). This crystalline phase, the product of a well characterized preparation, has been the subject of a number of investigations (*2*) and its formal stoichiometry has been generally accepted as Mg_4GeO_6 even though its crystal structure has not been determined. Both the magnesium germanate and the isomorphous fluorogermanate prepared by partial substitution of MgO by MgF_2 are effective as red-emitting phosphors when activated by tetravalent manganese. As part of a program to investigate the fluorescence efficiency of the manganese activator (*3*) we have prepared single crystals and determined the crystal structure of magnesium germanate.

Experimental

Preparation and Analysis

The magnesium germanate was prepared by standard ceramic techniques. Magnesium oxide (Mallinckrodt Chemical Co.) and germanium dioxide (Electronic Grade, Kawecki Chemical Co.) in a 4:1 mole ratio, with one mol% of manganese carbonate (Fisher Chemical Co.) added as a phosphor activator, were mixed and ground in acetone. After removal of the acetone at 110°C, the mixture was fired in air in a platinum crucible at 1100°C for 1 hr, reground and fired for 16 hr at 1200°C.

Suitable crystals were grown from a lead oxide (Fume Litharge, Evans Lead Co.) flux. A mixture of 75-g lead oxide and 27-g magnesium germanate in a 50-cc platinum crucible was heated at 1300°C for 4 hr in a silicon carbide resistance furnace. It was then cooled at about 4°/hr to 900°C and removed from the furnace. Dry oxygen was passed through the furnace to protect the crucible. The crystals were separated from the flux by leaching with hot, dilute hydrochloric acid.

A semiquantitative emission spectrographic analysis of the flux grown magnesium germanate crystals revealed the following approximate weight percent impurities: manganese (0.1–1.0 wt%); platinum (0.1–1.0 wt%); lead (0.01–0.1 wt%); silicon (0.001–0.01 wt%); aluminum (0.001–0.01 wt%). Quantitative analysis was undertaken for manganese and germanium by flame emission spectroscopy, magnesium was accurately determined by neutron activation analysis, and a colorimetric analysis was

† Proctor and Gamble Fellow, 1969–1970.

developed for platinum. In weight percents, the crystal analyses were

Atom	Found	Calculated ($Mg_{28}Ge_{10}O_{48}$)
Mg	31.9	31.30
Ge	33.8	33.38
Mn	0.72	
Pt	0.67	

It is clear that the analytical results do not even approximately correspond to the magnesium–germanium ratio in the reported phase Mg_4GeO_6. In anticipation of the results of the structure analysis (vide infra), the calculated composition is recorded for the contents of the unit cell; the agreement with the observed data is excellent. The impurity levels correspond to 0.3 atom of manganese and 0.08 atom of platinum per unit cell.

A series of preparations and crystallizations were undertaken with the starting charge ratio of Mg/Ge varying from 6:1 to 2.8:1. No new phases were observed but, in every case, MgO crystals appeared with the germanate of the above composition. The amount of MgO in the product decreased systematically as the starting charge ratio decreased.

X-ray powder patterns were obtained on a high resolution Guinier camera for the ceramic preparation, $4MgO \cdot GeO_2$, and for selected single crystals of the germanate. Except for the presence of two lines from MgO in the ceramic sample, the two patterns were identical; they corresponded to a pattern given in an earlier report on the ceramic material (*1*).

X-ray Diffraction Data

The flux grown crystals of magnesium germanate appeared in thin tabular forms and in clusters of macroscopic intergrowth twins; individual crystals of millimeter dimensions were readily accessible. The pale yellow crystals fluoresced strongly under ultraviolet excitation with the red emission characteristic of tetravalent manganese. Because of the relatively high linear absorption coefficient of the material for MoK_α radiation, a specimen suitable for data collection was prepared by grinding a crystal to an accurate sphere, 0.019(1) cm in diameter.

The Laue symmetry and extinctions determined from Weissenberg and precession photographs established the space group to be either *Pbam* or *Pba2*. No measurable piezoelectric effect could be detected using a sensitive Giebe–Scheibe detector designed by H. Diamant; this supports, but does not confirm, the centrosymmetric *Pbam*.

The lattice parameters were determined in a PICK II least-squares refinement program, using 47 sets of measurements within the angular range $43° < |2\theta| < 64°$; the reflections were automatically centered on a Picker FACS-I four-circle diffractometer using MoK_{α_1} radiation. At 21°C the parameters are $a = 14.512(2)$, $b = 10.219(2)$, and $c = 5.944(1)$ Å where the figures in parentheses represent meaningful standard deviations in the last reported figure.

A density, $\rho_0 = 3.98(4)$ g/cc, was determined from a pycnometric measurement on a number of selected single crystals. With eight formula units per cell the calculated density is $\rho_c = 4.01$ g/cc for a composition Mg_4GeO_6, and it is $\rho_c = 4.10$ g/cc for $Mg_{3\cdot 50}Ge_{1\cdot 25}O_6$, the composition derived from the structure analysis. Considering the fact that the crystals contain small but visible voids, this agreement is entirely satisfactory.

The diffraction intensities were measured using Zr filtered MoK_α radiation at a take-off angle of 2.5° with the diffractometer operating in the θ–2θ scan mode. The scans were at 1° per min over 1.5° with allowance for dispersion, and with 40-sec background counts taken at both ends of the scan. Of 2191 independent data investigated in the angular range $2\theta \leq 71°$, a total of 2096 were retained objectively observed with $|F_0| > 0.670\sigma_F$, where σ_F is defined by

$$\sigma_F = 0.02|F_0| + \left[\frac{C + k^2 B}{(2|F_0|L_P)}\right]^{1/2}.$$

The total count from the scan is C, and k is the ratio of scanning time to the total background count B. Frequent monitoring of three reflections over the entire course of data collection showed no evidence of crystal degradation; indeed, less than 2% random variation in intensity was noted. The data were corrected for Lorentz and Polarization effects and absorption corrections (*4*) were applied for a spherical crystal with a linear absorption coefficient based upon the final stoichiometry determined from the structure analysis. With $\mu R = 0.89$, the maximum absorption corrections applied to any reflection was $4.0 \pm 0.5\%$ of $|F_0|$.

Determination of the Structure

Preliminary analysis revealed simple relationships among the lattice parameters which corresponded to a closest packed structure of oxygen atoms with six-

layer stacking along the a axis. With $a/c \simeq \sqrt{6}$, $b/c \simeq \sqrt{3}$, and c equal to twice the ionic diameter of oxygen, it is possible to demonstrate that only two stacking sequences conform to the symmetry requirements of *Pbam* or *Pba2*. The partial structural information contained in the two oxygen arrays, $(ABABAB)_n$ and $(ABACBC)_n$, was directly utilized in the interpretation of the Patterson synthesis of the diffraction data.

An analysis of intensity statistics indicated that the centrosymmetric space group, *Pbam* (*5*), was the most probable one and that the scale factor was approximately 1.1. Two modified Patterson syntheses were calculated with coefficients based upon the difference between the observed structure factors and those calculated for each of the two oxygen arrays. Only the synthesis for the sequence $(ABACBC)_n$ showed a significant reduction in the number of peaks; the remaining metal–metal vectors were readily interpretable and yielded the positions of three germanium atoms. Successive difference Fourier syntheses, phased with these three atoms in *Pbam*, reproduced the entire structure.

Refinement of the Structure

An initial cycle of full-matrix least-squares (*6*) refinement yielded a standard residual

$$R = \Sigma||F_0| - |F_c||/\Sigma|F_0| = 0.10,$$

but the isotropic thermal parameters for the germanium atoms were negative. It was clear from the results of a second cycle, based upon data with $\sin\theta/\lambda \geqslant 0.20$, that extinction corrections were required; an algorism for isotropic extinction was formulated on the basis of Zachariasen's recent analysis (*7*) and incorporated into the least-squares program. In the final refinement, the maximum extinction correction was 26.7% of $|F_c|$ for the 004 reflection.

In the final refinement, each reflection was weighted by employing a four-term power series in $|F_0|$ with coefficients determined by minimizing the function

$$R = \sum_H (\Delta|F_H| - \sum_i^4 a_i|F_H|^i)^2.$$

Scattering factors for Mg^+ were interpolated from

TABLE I

FRACTIONAL ATOMIC COORDINATES AND THERMAL PARAMETERS[a, b]

Atom	Point Symmetry (*5*)	$10^4 x$	$10^4 y$	$10^4 z$	B[c]
Ge(I)	2/*m*	0	0	0	0.30(1)
Ge(II)	*m*	1256.3(3)	5015.6(5)	0	0.28(1)
Ge(III)	*m*	1862.3(3)	3250.9(5)	0.5	0.39(1)
Mg(I)	2/*m*	0	0.5	0.5	0.39(3)
Mg(II)	2/*m*	0	0	0.5	0.42(3)
Mg(III)	*m*	1759(1)	1785(2)	0	0.39(2)
Mg(IV)	*m*	3259(1)	1466(2)	0.5	0.36(2)
Mg(V)	*i*	−46(1)	2517(1)	2423(2)	0.38(2)
Mg(VI)	*i*	3315(1)	4192(1)	2460(2)	0.37(2)
O(I)	*m*	840(2)	3374(3)	0	0.38(4)
O(II)	*m*	4217(2)	3488(3)	0	0.35(4)
O(III)	*m*	2520(2)	34(4)	0	0.43(4)
O(IV)	*m*	677(2)	3294(4)	0.5	0.48(5)
O(V)	*m*	4129(2)	3315(3)	0.5	0.37(4)
O(VI)	*m*	2562(2)	−231(3)	0.5	0.45(4)
O(VII)	*i*	757(2)	780(2)	2234(4)	0.42(3)
O(VIII)	*i*	4142(2)	810(2)	2482(4)	0.38(3)
O(IX)	*i*	2426(2)	2513(2)	2731(4)	0.45(3)

[a] Numbers in parentheses are estimated standard deviations in last significant figure.

[b] Coordinates of 0 or 0.5 are determined by site and space group symmetry.

[c] Isotropic thermal parameter obtained from least-squares refinement of model with isotropic thermal parameters.

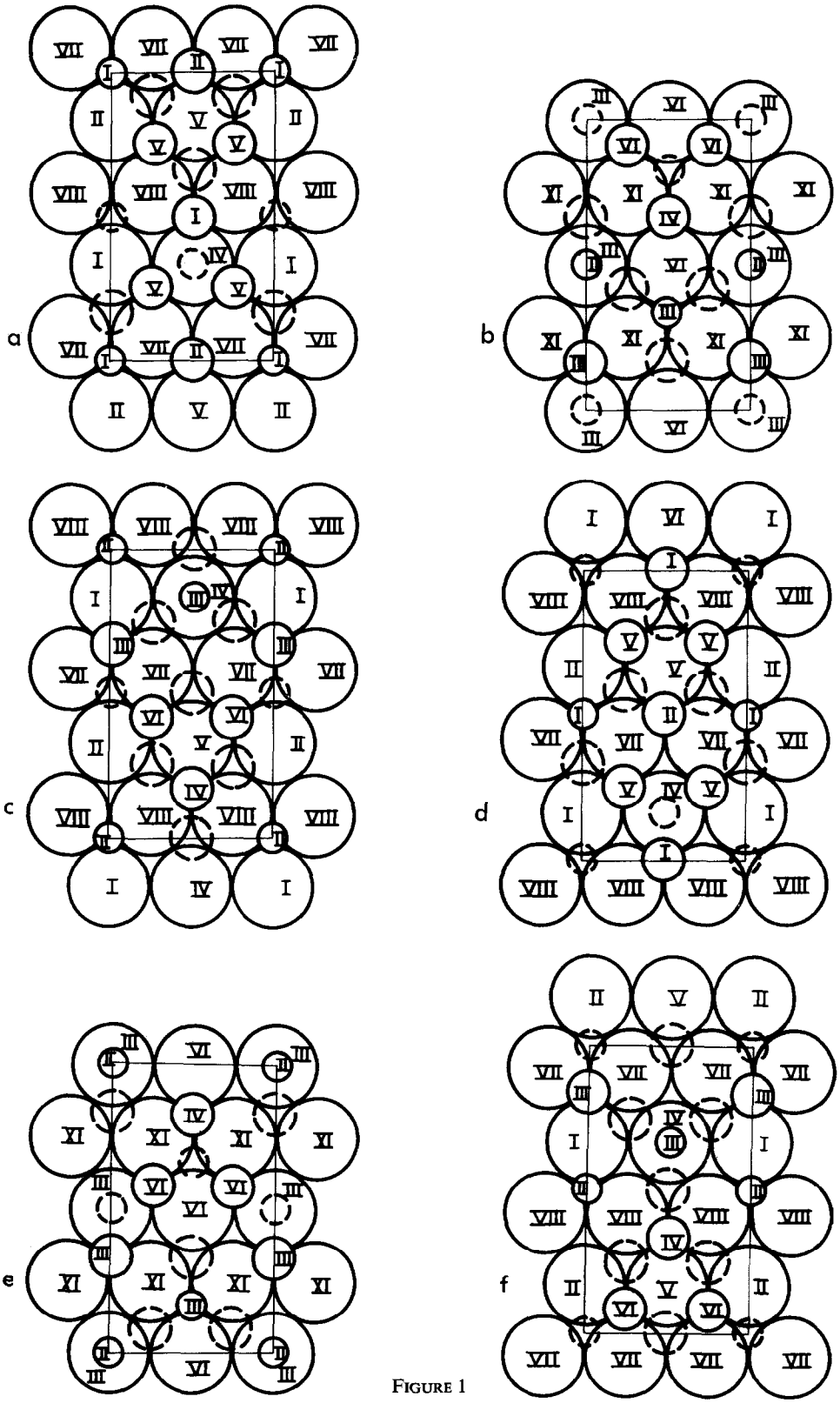

FIGURE 1

TABLE II

BOND DISTANCES, POLYHEDRAL EDGE LENGTHS, AND BOND ANGLES FOR GERMANIUM ATOMIC POSITIONS[a]

Atoms	Distance, Å	Atoms	Angle, degrees
Ge(I)–O(II)	1.918(3)	O(II)–Ge(I)–O(VII)	89.7(1)
Ge(I)–O(VII)	1.899(2)	O(II)–Ge(I)–O(VII)	90.3(1)
O(II)–O(VII)	2.693(4)	O(VII)–Ge(I)–O(VII)	88.7(1)
O(II)–O(VII)	2.706(4)	O(VII)–Ge(I)–O(VII)	91.3(1)
O(VII)–O(VII)	2.656(5)	O(VII)–Ge(I)–O(VII)	180.0
O(VII)–O(VII)	2.715(5)		
Ge(II)–O(I)	1.783(3)	O(I)–Ge(II)–O(III)	110.4(2)
Ge(II)–O(III)	1.776(3)	O(I)–Ge(II)–O(VIII)	108.6(1)
Ge(II)–O(VIII)	1.780(3)	O(III)–Ge(II)–O(VIII)	108.6(1)
O(I)–O(III)	2.922(5)	O(VIII)–Ge(II)–O(VIII)	112.0(2)
O(I)–O(VIII)	2.991(4)		
O(III)–O(VIII)	2.888(4)		
O(VIII)–O(VIII)	2.950(5)		
Ge(III)–O(IV)	1.720(3)[b]	O(IV)–Ge(III)–O(VI)	116.8(2)
Ge(III)–O(VI)	1.762(4)	O(IV)–Ge(III)–O(IX)	118.6(1)
Ge(III)–O(IX)	1.748(2)	O(VI)–Ge(III)–O(IX)	99.1(1)
O(IV)–O(VI)	2.967(5)	O(IX)–Ge(III)–O(IX)	100.9(2)
O(IV)–O(IX)	2.983(4)		
O(VI)–O(IX)	2.670(4)		
O(IX)–O(IX)	2.697(5)		

[a] Numbers in parentheses are estimated standard deviations in last significant figure.

[b] "Axial" bond.

tables (*8*) for Mg° and Mg^{2+} and standard factors (*9*, *8*) were used for Ge^{2+} and O^{-}; anomalous scattering terms (*10*) were also included for germanium. The sensitivity of the final results to the detailed form of the scattering functions was tested by substituting the scattering factors for Mg°, Ge°, and 0° in a refinement cycle; no statistically significant changes were noted in any of the refined parameters.

With isotropic thermal parameters for all atoms, the final full-matrix least-squares refinement included 38 independent data for each of the 55 parameters. With this unusually high data–parameter ratio, a standard residual, $R = 0.051$, was obtained at convergence; the corresponding weighted residual, $R_w = 0.062$. With anisotropic thermal parameters for all atoms, the standard residual was reduced to 0.044.[1]

The resulting thermal parameters gave no indication of local disorders or of partial occupancies of specific sites. To verify this conclusion, an additional refinement cycle was performed with variable occupancy parameters for the metal atoms; no significant changes were noted. The final atomic coordinates and thermal parameters are presented in Table I.

FIG. 1. The structure of magnesium germanate. The unit cell contents, $Mg_{28}Ge_{10}O_{48}$, are shown relative to the six-layer stacking sequence of oxygen $(ABACBC)_n$. Each oxygen layer parallel to (100) is shown in large circles; the smallest circles represent germanium ions and the intermediate circles are magnesium ions. For each layer, those metal ions that lie above the oxygen plane are shown with full circles; for aid in visualization of the stacking of the successive layers (*a*), (*b*), (*c*), (*d*), (*e*), and (*f*), the metal ions that lie below the oxygen plane, and thereby belong to the subsequent layer of structure, are indicated in broken circles. The Roman numerals identify all symmetry related sets of atoms and correspond to the labels in the text and tables.

[1] A table of $|F_0|$ and $|F_c|$ has been deposited as Document number 1108 with the ADI Auxiliary Publications Project, Photoduplication Service, Library of Congress, Washington 25, D.C. A copy may be secured by citing the Document number and by remitting $5.00 for photoprints, or $2.00 for 35-mm microfilm. Advance payment is required. Make checks or money orders payable to: Chief, Photoduplication Service, Library of Congress.

Discussion

The stoichiometry of the magnesium germanate prepared in this study is unambiguously determined by the crystal structure analysis. The high quality of the diffraction data, the detailed refinement procedures, and the excellent statistical figures of merit leave little room for doubt that the contents of the unit cell are $Mg_{28}Ge_{10}O_{48}$. Moreover, this stoichiometry, $Mg_{14}Ge_5O_{24}$, is strongly supported by the analytical results on selected single crystals. Writing it as $Mg_{3.50}Ge_{1.25}O_6$, it can be seen that it differs markedly from the reported composition, Mg_4GeO_6. Since there is no evidence for the existence of a second phase in the preparation, it seems unlikely that the composition Mg_4GeO_6 exists.

The crystal structure is most simply described as a stacking of six oxygen–metal ion layers along the *a* axis; the close packed oxygen layers are stacked in the sequence $(ABACBC)_n$. The oxygen–metal ion layers are depicted in Fig. 1. Closer examination of the layers reveals that the structure involves the alternate stacking of layers of two substructures, each of which is derivative from a well known structure.

The first layer, shown in Fig. 1(a) is derived from the magnesium oxide structure. In (111) of MgO, all of the octahedral sites are filled with magnesium ions; in the present case, alternate rows of magnesium ions parallel to the (100) face diagonal have either a germanium ion or a vacancy in every fourth site. The composition of the substituted MgO layer is, therefore, Mg_6GeO_8.

Taken together, the next two oxygen–metal ion layers, Fig. 1(b) and (c), constitute a compound layer which is exactly one unit cell of an olivine structure with the composition Mg_2GeO_4. In complete analogy to olivine, the bivalent magnesium atoms occupy the octahedral positions and the tetravalent germanium atoms occupy the tetrahedral positions. The magnesium germanate structure is then completed with a second MgO-type layer, as shown in Fig. 1(d), and a second olivine-type layer, as in Fig. 1(e) and (f). The olivine layers are so situated that, at each interface the occupied tetrahedral positions share a face with the vacant octahedral positions in the MgO-type layers.

At first glance, this successive alternation of olivine layers with layers of a second structural type is reminiscent of the stacking in the silicate structures of the olivine group, such as norbergite, humite and chondridite (*11*). However, in the present case, the olivine layer is strikingly different in that it is derived from a layer perpendicular to the *b* axis in the basic olivine structure rather than from a layer perpendicular to the *c* axis, as is the case for the silicate structures. Thus, the *a* glide plane in the basic olivine structure (*Pnma*) corresponds to the *b* glide plane in the present structure. This propensity of olivine for forming compound structures suggests that analogous structures might exist in the silicate system.

The foregoing description was based upon an idealized closest packed oxygen anion structure; in fact, a number of the tetrahedral and octahedral metal atom sites display considerable deviation from

TABLE III

BOND DISTANCES AND POLYHEDRAL EDGE LENGTHS FOR THE MAGNESIUM ATOMIC POSITIONS[a]

Atoms	Distance, Å	Atoms	Distance, Å
Mg(I)–O(IV)	2.001(4)	Mg(II)–O(V)	2.136(3)
Mg(I)–O(VIII)	2.116(2)	Mg(II)–O(VII)	2.132(2)
O(IV)–O(VIII)	2.836(4)	O(V)–O(VII)	3.012(4)
O(IV)–O(VIII)	2.986(4)	O(V)–O(VII)	3.023(4)
O(VIII)–O(VIII)	2.950(5)	O(VII)–O(VII)	2.656(5)
O(VIII)–O(VIII)	2.991(4)	O(VII)–O(VII)	2.715(5)
Mg(III)–O(I)	2.101(4)	Mg(IV)–O(V)	2.273(4)
Mg(III)–O(III)	2.103(4)	Mg(IV)–O(VI)	2.008(4)
Mg(III)–O(VII)	2.220(3)	Mg(IV)–O(VIII)	2.081(3)
Mg(III)–O(IX)	2.032(3)	Mg(IV)–O(IX)	2.103(3)
O(I)–O(VII)	2.967(4)	O(V)–O(VIII)	2.966(4)
O(I)–O(IX)	2.951(4)	O(V)–O(IX)	2.932(4)
O(III)–O(VII)	2.981(4)	O(VI)–O(VIII)	2.937(4)
O(III)–O(IX)	3.012(4)	O(VI)–O(IX)	2.670(4)
O(VII)–O(VII)	2.715(5)	O(VIII)–O(VIII)	2.950(5)
O(VII)–O(IX)	3.015(3)	O(VIII)–O(IX)	3.041(3)
O(IX)–O(IX)	2.697(5)	O(IX)–O(IX)	2.697(5)
Mg(V)–O(I)	2.120(3)	Mg(VI)–O(II)	2.091(3)
Mg(V)–O(II)	2.067(3)	Mg(VI)–O(III)	2.085(3)
Mg(V)–O(IV)	2.019(3)	Mg(VI)–O(V)	2.116(3)
Mg(V)–O(V)	2.122(3)	Mg(VI)–O(VI)	2.060(3)
Mg(V)–O(VII)	2.127(3)	Mg(VI)–O(VII)	2.113(3)
Mg(V)–O(VIII)	2.077(2)	Mg(VI)–O(IX)	2.152(3)
O(I)–O(II)	3.028(5)	O(II)–O(III)	2.975(5)
O(I)–O(IV)	2.9825(7)	O(II)–O(V)	2.9799(7)
O(I)–O(VII)	2.967(4)	O(II)–O(VII)	2.693(4)
O(I)–O(VIII)	2.991(4)	O(II)–O(IX)	3.222(4)
O(II)–O(V)	2.9799(7)	O(III)–O(VI)	2.9849(7)
O(II)–O(VII)	2.706(4)	O(III)–O(VII)	2.981(4)
O(II)–O(VII)	3.111(4)	O(III)–O(IX)	3.046(4)
O(IV)–O(V)	2.784(5)	O(V)–O(VI)	2.869(5)
O(IV)–O(VII)	3.052(4)	O(V)–O(VII)	3.012(4)
O(IV)–O(VIII)	2.836(4)	O(V)–O(IX)	2.932(4)
O(V)–O(VII)	3.012(4)	O(VI)–O(VII)	3.260(4)
O(V)–O(VIII)	2.966(4)	O(VI)–O(IX)	2.670(4)

[a] Numbers in parentheses are estimated standard deviations in the last significant figure.

TABLE IV

SELECTED BOND ANGLES (DEGREES) FOR THE MAGNESIUM ATOMIC POSITIONS[a]

Atom	$(O-M-O)_{max}$	$(O-M-O)_{min}$
Mg(I)	93.0(1)	87.0(1)
Mg(II)	100.9(1)	79.1(1)
Mg(III)	106.1(2)	73.5(1)
Mg(IV)	98.6(1)	79.7(1)
Mg(V)	97.3(1)	80.3(1)
Mg(VI)	102.7(1)	78.7(1)

[a] Numbers in parentheses are estimated standard deviations in last significant figure.

the idealized geometry. The octahedral coordination around Ge(I) is quite regular, as is the tetrahedron around Ge(II); as shown in Table II, the polyhedral angles are within 2.5° of the ideal values and all M–O are equal (±0.01 Å) within each polyhedron. The tetrahedral geometry around Ge(III) is distinctly trigonal pyramidal. The O(IX)–O(VI)–O(IX) face of this tetrahedron has three edges (2.68 Å av) which are shared with three magnesium occupied tetrahedra. The other three edges average 2.98 Å in length as compared to the 2.94 Å av around Ge(II).

In an idealized array with an O–O distance of 2.96 Å, the M–O distances would be 2.09 Å for the octahedral positions and 1.81 Å for the tetrahedral positions. All of the germanium–oxygen distances are considerably foreshortened, especially around the octahedral Ge(I) where the average is 1.91 Å. The quasithreefold axial bond, Ge(III)–O(IV) = 1.72 Å, is the shortest metal–oxygen distance in the structure. It is undoubtedly a result of the proximity of the three magnesium octahedra with an average Mg–Ge separation of 2.74 Å.

The coordination octahedra around the magnesium atoms are markedly irregular. The Mg–O distances vary 2.00–2.27 Å, the O–O distances range 2.656–3.111 Å and the O–Mg–O angles deviate as much as 16° from the ideal value of 90°. Nevertheless, the O–O distances average about 2.95 Å and the Mg–O distances are approximately the sum of the ionic radii, 2.10 Å (*12*); the detailed distances are presented in Table III. A measure of the distortion of the octahedra appears in the angles given in Table IV.

With a single exception, each oxygen atom is bound to one germanium atom; O(V) is unique in that it is surrounded by an octahedral arrangement of magnesium atoms. Each of the six oxygen atoms bound to Ge(I) are surrounded by four magnesium ions and one germanium ion; a vacant cation site opposite the germanium atom completes the octahedral array. Apparently, the high charge on the germanium ion is sufficient to polarize the oxygen ions and stabilize the structure. A similar arrangement is associated with the anion coordination group around the Mn^{4+} ion in the Mg_6MnO_8 structure (*13*). The surroundings of the four oxygen atoms bound to Ge(II) and the axial oxygen atom bound to Ge(III) are nearly isonomous; each is associated with three magnesium atoms at the face of a somewhat elongated tetrahedron with a germanium atom at the opposite vertex.

Acknowledgments

We thank Dr. J. Roth of the Materials Science Center's Analytical Facility for the analyses. This work was supported by the Advanced Research Projects Agency through the Materials Science Center, Cornell University, Ithaca, New York.

References

1. C. R. ROBBINS AND E. M. LEVIN, *Amer. J. Sci.* **257**, 63 (1959).
2. See F. A. KROEGER AND J. VAN DEN BOOMGAARD, *J. Electrochem. Soc.* **97**, 377 (1950); G. KEMENY AND C. H. HAAKE, *J. Chem. Phys.* **33**, 783 (1960) and references therein.
3. L. THORINGTON, *J. Opt. Soc. Amer.* **40**, 579 (1950).
4. "International Tables for X-Ray Crystallography," Mathematical Tables, Vol. II, p. 302, The Kynoch Press, Birmingham, England, 1968.
5. "International Tables for X-Ray Crystallography," Symmetry Groups, Vol. I, p. 143, The Kynoch Press, Birmingham, England, 1968.
6. W. R. BUSING, K. O. MARTIN, AND H. A. LEVY, "ORFLS, A Fortran Crystallographic Least-Squares Program," ORNL-TM-305, Oak Ridge National Laboratory, Oak Ridge, Tennessee, 1962.
7. W. H. ZACHARIASEN, *Acta Crystallogr.* **23**, 558 (1967); *Sect. A* **24**, 324 (1968).
8. D. T. CROMER AND J. B. MANN, *Acta Crystallogr.* **24**, *Sect. A* **24**, 321. (1968).
9. "International Tables for X-Ray Crystallography," Physical and Chemical Tables, Vol III, p. 204, The Kynoch Press, Birmingham, England, 1968.
10. D. T. CROMER, *Acta Crystallogr.* **18**, 17 (1965).
11. W. H. TAYLOR AND I. WEST, *Proc. Roy. Soc. Ser. A* **117**, 517 (1928); *Z. Kristallogr.* **70**, 461 (1929).
12. V. M. GOLDSCHMIDT, "Geochemistry," Clarendon Press, Oxford, 1952.
13. J. S. KASPER AND J. S. PRENER, *Acta Crystallogr.* **7**, 246 (1957).